Uncertainty-Adjusted Benefit–Cost Analysis of Urban Heatwave Adaptation Technologies under Climate Change: Evidence from 229 Korean Municipalities

Sangmin Lee, Wooyoung Choi, Yewon Choi, Donghwi Kim*, Donghwan An **, Kwansoo Kim ***

Abstract

Normally benefit–cost analysis of climate adaptation counts only the reduction in expected damages, leaving the value of reduced uncertainty uncounted. We extend the appraisal of urban heatwave adaptation to include this additional channel reflecting the fat-tail phenomenon of climate change. Defining utility over damages, we derive the risk premium from the first two conditional moments and obtain the marginal risk premium benefit (MRPB) by differentiating it with respect to the technology stock, since an additional unit shifts both the mean and the variance of damages. Using a panel of all 229 Korean municipalities for 2016–2022, we estimate conditional mean and variance equations for four technologies—cooling fog, cool roofs, green roofs and walls, and shade canopies—and recover benefit–cost ratios to 2050 under four SSP scenarios. All four reduce the conditional variance of damages, and the MRPB amounts to 18.7 to 61.8 percent of the conventional marginal benefit, which only focuses on the mean effects. Incorporating the MRPB as an additional benefit, the number of technologies passing the benefit–cost test is found to be from one to two over the observation period, with cool roofs moving from 0.976 to 1.158, and to three in the projection horizon. The adjustment leaves the ranking of technologies within a region unchanged but widens the gap across emissions pathways, which is 1.3 to 1.4 times on expected benefits alone and 2.3 to 2.6 times once risk associated with climate change is priced. We demonstrate that appraisals that omit the cost of risk therefore understate the value of adaptation, particularly where mitigation is delayed.

Keywords: heatwave adaptation; benefit–cost analysis; risk premium; conditional variance; SSP scenarios

[*] Graduate Students, at Department of Agricultural Economics and Rural Development, College of Agriculture and Life Sciences, Seoul National University

[**] Professor, College of Agriculture and Life Sciences, Seoul National University, email: dha@snu.ac.kr

[***] Corresponding Author, Professor, College of Agriculture and Life Sciences, Seoul National University, email: kimk@snu.ac.kr

1. Introduction

Rising damages from extreme heat have drawn growing attention to heat adaptation technologies, in large part because a substantial share of the health burden appears amenable to technological solutions (Barreca et al., 2016). Against this backdrop, Korean local governments have begun deploying a range of urban heat adaptation measures, including green roofs and walls, cooling fog systems, cool roofs, and shade canopies (Lee and Cho, 2024; Pyon, 2022). Economic feasibility analysis of this kind is conventionally done through benefit-cost analysis. In the United States, OMB(Office of Management and Budget) Circular A-4 sets out the standard procedure for appraising public investment; the United Kingdom does so through His Majesty's (HM) Treasury's Green Book, and Korea's preliminary feasibility study guidelines follow the same framework.

Such analyses, however, typically count only the expected benefits a technology delivers, leaving aside any benefits from the reduction in uncertainty itself. This practice has long found support in Arrow and Lind (1970): when the risk of a public investment is spread across a large body of taxpayers, the burden borne by any one of them becomes negligible, so the government may reasonably act as though she were a risk neutral. Yet a body of work has questioned whether governments—national or local—are in fact risk neutral. Disaster losses constitute a contingent liability of the public sector, and once losses exceed what available resources can absorb, the Arrow-Lind result no longer holds (Hochrainer-Stigler et al., 2018). Empirical evidence is consistent with this view: disasters have been shown to significantly weaken the fiscal balance and own-source revenues of local governments (Wiyanti and Halimatussadiah, 2021).

There is a further reason to account for a risk premium in the case of extreme events such as heat waves, namely the thickness of the tail of the damage distribution. While aggregate and mean damages from natural disasters have grown only modestly, their distributions have become markedly more right-skewed and fat-tailed, with the sharpest increases concentrated in the upper quantiles (Coronese et al., 2019). When the tail is thick, an evaluation resting on expected values understates the welfare consequences for a risk-averse decision maker, and the appropriate shadow price for policy is the certainty equivalent which takes the value of risk into account rather than the expected value (Weitzman, 2009; Newbold et al., 2013).

Methods for incorporating risk aversion into benefit-cost analysis are themselves well developed. Markandya et al. (2019) derive region-specific risk premia from the means and variances of climate damage distributions, embed them in the damage function of an integrated assessment model, and find that both mitigation and adaptation spending rise substantially as a result. Kind et al. (2016, 2017) develop a welfare framework grounded in the certainty equivalent and show, in a flood risk application, that the ranking of flood defense projects shifts once the risk premium is taken into account.

Within the disaster risk literature, a related approach partitions losses into risk layers according to their size relative to the government's fiscal capacity and assigns distinct financing instruments to each layer (Mechler et al., 2010; Hochrainer-Stigler et al., 2018). A separate literature, rooted in production economics, has developed methods for separately identifying how an input affects the mean and the variance of output. The stochastic production function of Just and Pope (1978) specifies mean and variance equations separately, making it possible to classify inputs as risk-increasing or risk-decreasing, and Antle (1983) generalized this into a moment-based approach. Within this framework, the benefit of a risk-decreasing input decomposes into a reduction in expected loss and a reduction in the cost of bearing risk. In this line of research, Kim and Chavas (2003) applied the framework to the risk-management consequences of technical change. And a number of empirical studies have found that the risk-reducing effect of a technology can contribute to welfare on a scale comparable to its effect on the mean (Traxler et al., 1995; Di Falco and Chavas, 2009).

The two strands have rarely been brought together. Work on risk premium generally takes the damage distribution as given and does not explicitly model the channel through which a policy or technology alters that distribution. The moment-based approach does estimate the variance effects of inputs and translates them into a risk premium, but it has been applied primarily to agricultural production decisions and only rarely carried through to the benefit-cost analysis of public investment.

This gap is evident in Choi et al. (2026), who estimate the benefits of four urban heat adaptation technologies across all 229 Korean municipalities, linking technology stocks to damages through a heat wave resilience index and recovering the marginal benefit of each technology. As is conventional, benefits in their study are measured entirely by the reduction in expected damages: the second moment of the damage distribution plays no role, and the resulting benefit-cost ratios are therefore applicable to a risk-neutral social planner. The present paper takes up what that exercise set aside. We retain the mean equation and the marginal benefit calculation of that study and ask how the benefit-cost ratios change once the conditional variance of damages, and the social planner's risk aversion preference to these damages, are brought into the accounting.

Our analysis proceeds in four steps. First, we specify a utility function over damages, derive the certainty equivalent and the associated risk premium, and obtain the “marginal” risk premium benefit (MRPB) by totally differentiating the risk premium with respect to the technology stock. We focus on the fact that the technology shifts both the conditional mean and the conditional variance. Second, using panel data on all 229 Korean municipalities for the period 2016–2022, we estimate a conditional mean equation and a conditional variance equation for heat damages. Because adaptation technologies affect damages through a heat wave resilience index (HWRI), the two stages are linked by the chain rule. Following the moment-based approach (Antle, 1983), the conditional variance is estimated from the residuals of the mean equation. Third, we combine the two sets of estimates to obtain the marginal risk premium benefit for each technology, add it to the conventional marginal benefit, and recompute benefit-cost ratios. Fourth, we project benefit-cost ratios through 2050 under SSP scenarios and examine their sensitivity to the coefficient of risk aversion.

The paper makes two contributions. First, it monetizes the reduction in the risk premium attributable to adaptation technologies and incorporates it into the benefit-cost ratio analysis. Whereas the existing literature has largely focused on the level of the risk premium (in an average sense), we compute a risk benefit tied to the marginal effect of the technology (in a marginal sense), yielding a measure that can inform judgments about the economic merit of "a unit increase" of individual technologies. Second, we find that accounting for the cost of risk can change whether a technology passes the benefit-cost test, which suggests that counting only the reduction in expected damages may understate the value of adaptation investment.

The remainder of the paper is organized as follows. Section 2 lays out the theoretical framework for the risk premium and the marginal risk premium benefit. Section 3 describes the econometric model and the data, and Section 4 presents the estimation results and benefit-cost ratios. Section 5 reports projections by SSP scenarios along with sensitivity analysis, and Section 6 concludes with a discussion of policy implications.

2. Data

2.1. Data construction

2.1.1. Observed data

Motivated by Choi et al. (2026), this study adopts a municipality-year panel structure covering 229 cities, counties, and districts in South Korea over 2016–2022. The observed dataset combines heatwave-related economic damage, meteorological conditions, heatwave adaptation technologies, and local resilience indicators. The municipality-year structure captures both cross-sectional differences in local exposure and resilience and temporal changes in heatwave conditions.

Table 1. Main input data and sources

Data	Items	Source
Heat-related medical expenditures	city/county/gu, inpatient/outpatient classification, number of patients, claims, and total cost of care for T67: heat and light effects	Claimed data from the Health Insurance Review and Assessment service (HIRA) (https://www.hira.or.kr)
Meteorological variables	Number of days with a daily maximum temperature of 33°C or higher	Korea Meteorological Administration (KMA) Open MET Data Portal (https://data.kma.go.kr)
Wages and number of workers	Number of workers and wage by industry & city	Ministry of Employment and Labor (MOEL), Business labor force survey

			(https://laborstat.moel.go.kr)

Note: All collection periods range from 2016 to 2022. Indicator classification and data source selection were adapted from choi et al. (2026).

Heatwave-related damage is defined as the sum of direct medical expenditures associated with heat-related illness and indirect labor-productivity losses attributable to excessive heat. Medical expenditures are constructed from Health Insurance Review and Assessment Service (HIRA) claims for T67 (effects of heat and light). Labor-productivity losses are estimated using Wet-Bulb Globe Temperature (WBGT) together with industry-specific employment and wage information, thereby converting heat-induced reductions in labor capacity into monetary losses. This measure therefore captures both health-related expenditures and a major economic consequence of heat exposure.

Meteorological data are obtained from the Korea Meteorological Administration (KMA) and matched to municipalities. The main weather variable used in the empirical analysis is the annual number of heatwave days, defined as days with a daily maximum temperature of 33°C or higher. This measure is consistent with the official KMA heatwave criterion and is also available under the same definition in the SSP climate projections. Using the same definition allows the observed heatwave-day series through 2022 to be consistently extended with SSP-based projections from 2023 onward.

The primary technology measures represent the cumulative deployment of four heatwave adaptation technologies: cooling fog systems, cool roofs, green roofs and walls, and shade canopies. Installation information is collected at the municipality-year level, and cumulative measures are used because installed facilities continue to provide heat-mitigation services beyond the year of installation. Cooling fog systems and shade canopies are measured by the cumulative number of facilities, whereas cool roofs and green roofs and walls are measured by cumulative installed area.

Local climate resilience is represented by the Heatwave Resilience Index (HWRI), which summarizes a municipality's capacity to cope with and reduce heatwave-related risks. The index consists of two components: adaptive capacity and vulnerability-reduction capacity. Adaptive capacity reflects the local resources and capabilities available to respond to and recover from heatwave impacts, whereas vulnerability-reduction capacity captures conditions that lower underlying exposure and sensitivity to heat-related risks. The two components incorporate indicators across economic, social, physical, governance, and human dimensions.

Table 2. Indicator configuration variables for Adaptive capacity

Sectors	Sub sectors	Variables	Sources
Economy	Economic Power	Amount of local tax per capita, financial independence rate, GRDP	Korean Statistical Information Service (Referred to as KOSIS) Regional Income (https://kosis.kr)

	Industry development	R&D expenditures per capita, number of researchers	Survey of R&D in Korea (https://kosis.kr)
Social	Medical response capability	Number of ambulances	Emergency Medical Services Statistics (https://kosis.kr)
		Number of hospitals/health centers/ medical personnel/emergency medical centers, health insurance subscribers	Korean Urban Statistics (https://stat.molit.go.kr)
		Number of hospital beds per 1,000 people	e-Regional Indicators of KOSIS
	Social infrastructure	Daily water consumption per capita, water supply rate, revenue water ratio	Korean Water Supply Statistics (https://www.water.or.kr)
	Energy	Energy use of buildings	Korean Urban Statistics
Physical Infra	Shelters of extreme heat	Number of welfare facilities for the aged, the homeless, the disabled, and children	Korean Urban Statistics
	Green infrastructure	Park area, green area, orchard area, forest area, stream area	Korean Urban Statistics
Governance	Budget	Amount of welfare budget	Local Finance Integrated Open System (https://www.lofin365.go.kr)
		Natural disasters management fund	KOSIS
	Response personnel	Population per 1 fire-fighting officer, number of officers (si-do)	Korean Urban Statistics

Note: Indicator classification and data source selection were adapted from choi et al. (2026).

Table 3. Indicator configuration variables for vulnerability-reduction capacity

Sectors	sub sectors	Variables	Sources
Economy	Industry development	Unemployment rate	Economically Active Population Survey from KOSIS
Social	Medical response capability	Unmet healthcare ratio	e-Regional Indicators from KOSIS
	Social infrastructure	Number of people under unmet water supply	Korean Water Supply Statistics
Human	Vulnerable populations	Population under 5 years of age, population of over 65 years of age, number of the disabled	Population Statistics Based on Resident registration of KOSIS
		Number of beneficiaries of national basic livelihood	Korean Urban Statistics

		Number of construction workers, number of skilled agricultural, forest, and fishery workers, number of grunt workers/temporary workers	Local Area Labor Force Survey (https://kosis.kr)
	Underlying disease	Number of people with hypertension, number of people with diabetes	Medical Service Usage Statistics by Region (https://kosis.kr)
	Population density	Population density	KOSIS
Physical Infra	Vulnerable facilities	Number of old buildings (20-24y/25-29y/30-34y/over 35y), road area, railroad area	Geospatial Information Platform (https://map.ngii.go.kr)
	Shelters of extreme heat	Number of welfare facilities for the aged, the homeless, the disabled, and children	Korean Urban Statistics
	Green infrastructure	Unexecuted Park area, paddy area, greenhouse area, upland field area	Korean Urban Statistics
	Density of buildings	Number of buildings, average height of buildings, average building coverage ratio, average building volume ratio	Geospatial Information Platform

Note: Indicator classification and data source selection were adapted from choi et al. (2026).

2.1.2. Future weather data

The observed panel is extended to 2050 using district-level climate projections from the KMA Climate Change Situation Map. The projections are based on the CMIP6[1] Shared Socioeconomic Pathway (SSP) framework, which combines alternative socioeconomic development pathways with different levels of future radiative forcing. Four scenarios are considered: SSP1-2.6, SSP2-4.5, SSP3-7.0, and SSP5-8.5[2]. Together, these scenarios represent a broad range of future climate conditions, from a relatively low-forcing sustainability pathway to a high-forcing fossil-fuel-based pathway. SSP4 is excluded because its adaptation-related socioeconomic conditions overlap closely with those represented by SSP3, whereas the selected four scenarios provide more clearly differentiated climate pathways (O'Neill et al., 2017; IPCC, 2021).

The KMA projections are downscaled to high spatial resolution and aggregated to administrative districts, allowing them to be matched to the 229 municipalities in the historical panel. Observed

1 CMIP6 refers to Phase 6 of the Coupled Model Intercomparison Project, an internationally coordinated framework under the World Climate Research Programme in which climate models from participating institutions are run under common experimental protocols. It provides the model basis for the IPCC Sixth Assessment Report.

2 SSP1-2.6 is a sustainability-oriented pathway with early and sustained mitigation; SSP2-4.5 continues current trends; SSP3-7.0 assumes regional fragmentation and weak mitigation; and SSP5-8.5 assumes fossil-fuel-intensive growth and the greatest warming.

weather data are retained through 2022, while SSP-based projections are used from 2023 to 2050. The annual number of heatwave days is measured consistently across the two periods as the number of days with a daily maximum temperature of 33°C or higher. This provides a common measure of heat exposure for linking historical observations with future projections.

In the projection exercise, heatwave exposure evolves according to each SSP pathway, while municipality-level HWRI and adaptation-technology stocks are held at their 2022 levels. This setup examines how the estimated benefits of the current level of adaptation change as heatwave exposure increases.

2.2. Descriptive statistics

Tables 4 and 5 summarize heatwave damage, the resilience index, and annual heatwave days over the observed period. Table 4 reports annual averages across municipalities. Damage averaged approximately USD 0.83 million per municipality over 2016–2022, but the annual figures diverge sharply. Damage peaked in 2018, the year with the highest average number of heatwave days in the sample, and fell to its lowest level in 2020, when exposure was also low. Both heat exposure and the damage associated with it thus vary considerably from year to year.

Table 4. Annual averages of key variables

Year	Heatwave damage[3] (USD)	HWRI	Average number of heatwave days (33°C)
2016	1,092,989	46.832	21.80
2017	531,450	45.569	14.15
2018	2,387,896	45.752	30.11
2019	618,841	45.253	13.06
2020	202,516	45.529	8386
2021	528,521	45.532	15.18
2022	462,307	46.790	13.64
Average	832,075	45.896	16.72

Note: HWRI = Adaptive Capacity Index + Vulnerability-Reduction Capacity Index. Damage and heatwave-exposure values are based on Choi et al. (2026).

Heatwave-related damage is relatively high in major urban and metropolitan regions, including Seoul, Daegu, Gyeonggi, and Daejeon, whereas Gangwon province (a province with large volume of

[3] Monetary values were converted from KRW to USD using an exchange rate of KRW 1.415.90 per USD.

rural mountainous areas) records the lowest average damage. At the same time, HWRI differs substantially across regions, with Gyeonggi (a province surrounding Seoul) and Seoul exhibiting particularly high levels. The coexistence of relatively high damage and high resilience in these regions suggests that high resilience does not necessarily imply low absolute damage where population and economic exposure are also large.

Table 5. Regional averages of key variables

Region	Heatwave damages (USD)	HWRI	Average number of heatwave days (33°C)
Seoul	1,725,349	51.846	19.86
Busan	858,458	45.462	10.30
Daegu	1,491,588	43.941	34.86
Incheon	880,934	42.767	11.21
Gwangju	1,027,907	43.428	25.74
Daejeon	1,039,730	44.639	19.80
Ulsan	794,718	42.027	6.48
Sejong	841,287	41.597	24.14
Gyeonggi	1,356,770	57.957	15.40
Gangwon	86,671	41.132	10.11
Chungbuk	431,209	42.575	19.74
Chungnam	613,474	43.034	15.71
Jeonbuk	468,440	41.773	15.87
Jeonnam	268,802	42.292	15.21
Gyeongbuk	508,806	42.969	20.47
Gyeongnam	860,060	43.451	18.99
Jeju	280,179	39.333	2.79
Average	796,140	44.131	57.579

Note: HWRI = Adaptive Capacity Index + Vulnerability-Reduction Capacity Index. Regional damage and heatwave-exposure values are based on Choi et al. (2026).

To examine how heatwave exposure changes under future climate conditions, Table 6 compares the distribution of annual heatwave days in the observed period with those projected under the four SSP scenarios. The mean number of annual heatwave days increases from 16.72 days during 2016–2022 to between 27.36 and 32.63 days during 2023–2050. The increase is also evident in the upper part of the distribution. The historical 95th percentile is 39 days, whereas the projected 95th percentile ranges from 48.8 days under SSP1 to 58.8 days under SSP5.

More importantly, heatwave conditions that were relatively uncommon during the historical period become considerably more frequent under the future scenarios. The share of municipality-year observations exceeding the historical 95th-percentile threshold increases from 5% in the observed period to 20.1% under SSP1 and 34.0% under SSP5. Similarly, the share exceeding the historical 99th-percentile threshold rises from 1% to between 9.7% and 22.2% across the SSP projections. These results indicate that future climate change is associated not only with a higher average level of heat exposure but also with a greater frequency of historically extreme heatwave conditions.

Table 6. Distribution of annual heatwave days in the observed period and SSP projections

Scenario	Period	Mean	SD	P95	P99	Max	Above observed P95 (%)	Above observed P99 (%)
Observed	2016-2022	16.72	11.65	39.0	45.0	55.0	5.0	1.0
SSP1-2.6	2023-2050	27.36	13.01	48.8	57.5	71.6	20.1	9.7
SSP2-4.5	2023-2050	30.23	12.98	51.3	61.1	72.6	25.5	12.5
SSP3-7.0	2023-2050	30.21	14.66	56.5	66.7	80.1	27.0	16.6
SSP5-8.5	2023-2050	32.63	15.29	58.8	66.7	76.4	34.0	22.2

Note: P95 and P99 denote the 95th and 99th percentiles of each scenario-specific distribution. The last two columns report the shares exceeding the historical P95 and P99 thresholds of 39 and 45 heatwave days, respectively.

Figure 1 provides a visual representation of these distributional changes using kernel density estimates. Compared with the observed distribution for 2016–2022, all four SSP distributions shift to the right, reflecting an overall increase in annual heatwave days. The projected distributions also extend farther into the upper range of heatwave exposure, with the shift becoming more pronounced under the higher-forcing scenarios. This pattern is consistent with the results in Table 6 showing that heatwave conditions located near the upper tail of the historical distribution become increasingly common under future climate scenarios demonstrating the fat-tailed phenomenon of climate change.

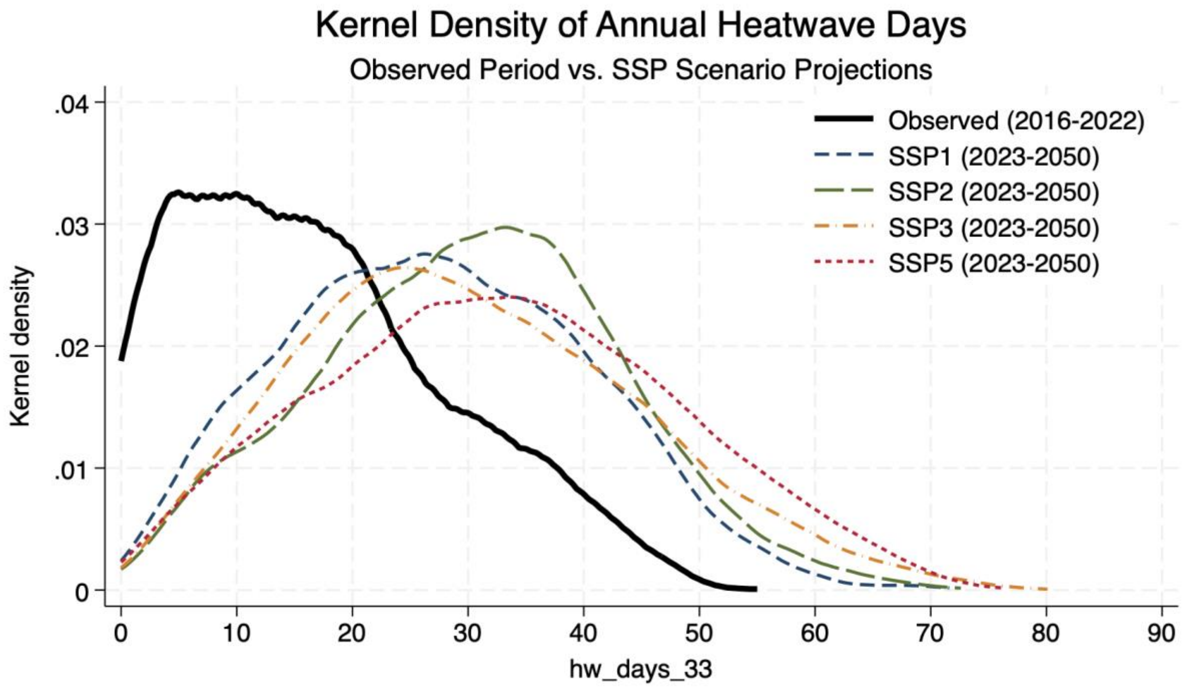

Figure 1. Kernel density of annual heatwave days: observed period and SSP scenario projections, 2023-2050. Source: Authors' calculations using KMA observed and SSP climate data.

3. Method

3.1 Conceptual framework

The framework discussed below evaluates the marginal benefit of each adaptation technology relative to its annualized cost. Section 3.1.1 defines the benefit-cost ratio and presents the conventional mean-based benefit measure, building on the specification adopted in the preceding study. Section 3.1.2 then extends this framework by introducing the risk premium and deriving the additional marginal benefit associated with reductions in damage variability.

3.1.1 Benefit-cost analysis

The benefit-cost ratio (BCR) is the standard criterion in the economic appraisal of public investment. In its conventional form, it expresses the total benefits of a project over a given period as a ratio of its total costs:

$$BCR = \frac{Total\ Benefit}{Total\ Cost} \tag{1}$$

A ratio above one means that benefits outweigh costs, and the project is judged economically feasible. So defined, however, the BCR measures an "average" effect suited to large-scale projects with dedicated budgets, whereas heatwave adaptation offers several coexisting options whose scale is itself a decision variable. Therefore, what matters here is the effect of an incremental unit of installation.

Let y_{it} denote the heat damage of municipality i in year t described in Section 2, and $\mu_{1,it} = E(y_{it})$ its conditional expectation. The marginal benefit of technology k, with technology adoption level $Tech_{k,it}$, is the reduction in expected damage from one additional unit increase in this technology,

$$Benefit_{k,it} \equiv -\frac{\partial \mu_{1,it}}{\partial Tech_{k,it}} \tag{2}$$

and, with c_k its equivalent annual cost — installation annualized over the service life plus maintenance — the "marginal" benefit-cost ratio is

$$BCR_{k,it} = \frac{Benefit_{k,it}}{c_k} \tag{3}$$

We take the marginal benefit from that study, which links technologies to damages through the Heatwave Resilience Index (HWRI) in two stages: technologies raise municipal resilience capacity, and higher capacity lowers damages. The econometric specification of the two stages — and the variance equation on which the risk premium in Section 3.1.2 rests — is set out in Section 3.2, and the annualized unit costs are likewise carried over.

This paper further monetizes the effect of each adaptation technology on the variance of damages, using the risk premium approach set out in Section 3.1.2, and reflects it as an additional benefit in the benefit-cost analysis. The uncertainty-adjusted ratio therefore adds this marginal risk premium benefit (MRPB) to the marginal benefit before dividing by cost:

$$BCR^{RA}_{k,it} = \frac{Benefit_{k,it} + MRPB_{k,it}}{c_k} \tag{4}$$

For a risk-neutral decision maker, the second term vanishes and (4) collapses to (3); the gap between the two ratios is the monetized value of uncertainty reduction, which mean-based appraisal leaves uncounted. This extended version of BCR is appropriate when the decision maker is not assumed to be a risk neutral (i.e., a risk-averse decision maker).

3.1.2 Risk premium

The approach developed here follows Kim and Chavas (2003), who measure the cost of bearing risk by the Pratt (1964) risk premium, approximate that premium from the conditional moments of the outcome distribution, and classify a technology as risk-increasing or risk-decreasing according to its effect on the premium. We transpose their framework from farm profit to municipal heat damage.

Uncertainty here refers to the variability of heat damages alone; risks in other disaster categories and fluctuations in municipal revenues stay outside the model. So long as those factors do not respond systematically to technology adoption, their omission leaves the estimated marginal risk premium benefit unaffected, since every object derived below is a derivative with respect to $Tech_{k,it}$ holding others constant.

Because the damage itself is the random variable of interest, utility as denoted by function *V*(.), is defined directly over damages rather than over income net of damages:

$$V(y) = -\frac{y^{1+\eta}}{1+\eta}, \qquad \eta > 0, \qquad V'^{(y)} < 0, \quad V''^{(y)} < 0 \tag{5}$$

Both signs matter. $V'(y) = -y^{\eta} < 0$ establishes damages as a bad thing: utility falls as they grow. $V''(y) = -\eta y^{\eta-1} < 0$ makes the function concave, so of two damage streams with the same mean, the more variable one is ranked worse. Concavity also delivers, through Jensen's inequality, $E[V(y)] \leq V(E[y])$; because $V(.)$ is decreasing with respect to y, the certain damage that yields the same utility as the uncertain damage must exceed the expected damage — the mark of a risk-averse evaluator. The parameter η is the curvature of (5): the elasticity $y\,\frac{V''(y)}{V'(y)} = \eta$ is constant, the same iso-elastic structure as the constant-relative-risk-aversion (CRRA) utility commonly specified over income or consumption, except that utility is decreasing rather than increasing because it is defined over damages. Constancy in relative terms implies that risk is assessed against the scale of damages — variability relative to the mean rather than in absolute size — which matters when municipalities of very different sizes are compared within a single framework.

Recall from Section 3.1.1 that $\mu_{1,it} = E(y_{it})$ denotes the conditional mean of damages. The certainty equivalent y_{it}^{*} is the certain damage level that gives the same utility as the uncertain damage, and the risk premium is its excess over the mean:

$$V(y_{it}^{*}) = E[V(y_{it})] \tag{6}$$

$$RP_{it} = y_{it}^{*} - \mu_{1,it} \tag{7}$$

RP_{it} is the maximum amount the municipality would pay, beyond expected damage, to have the variability removed — the money value of the risk it bears. Note that this is positive under risk aversion.

A second-order approximation turns (6) into a formula in the first two moments (Pratt, 1964). Let $\mu_{2,it} = E\left[\left(y_{it} - \mu_{1,it}\right)^{2}\right]$ denote the conditional variance. Expanding the left side of (6) to first order around $\mu_{1,it}$ gives

$$V(y_{it}^{*}) \approx V\left(\mu_{1,it}\right) + V'\left(\mu_{1,it}\right) \cdot RP_{it},$$

while expanding the right side to second order in y_{it} and taking expectations eliminates the first-order term:

$$E[V(y_{it})] \approx V\left(\mu_{1,it}\right) + \frac{1}{2} V''\left(\mu_{1,it}\right)\mu_{2,it}.$$

Equating the two and solving for the premium yields $RP_{it} = \frac{1}{2} \cdot \frac{V''(\mu_{1,it})}{V'(\mu_{1,it})} \cdot \mu_{2,it}$, and since $\frac{V''(\mu_{1,it})}{V'(\mu_{1,it})} =$

$\frac{-\eta\mu_{1,it}^{\eta-1}}{-\mu_{1,it}^{\eta}} = \frac{\eta}{\mu_{1,it}}$ under (5),

$$RP_{it} = \frac{\eta}{2} \cdot \frac{\mu_{2,it}}{\mu_{1,it}}. \tag{8}$$

Since μ_2 carries squared monetary units and μ_1 monetary units, the premium measured in monetary units: it is proportional to the variance of damages and inversely proportional to their expected level — equivalently, proportional to $\mu_{1,it}$ times the squared coefficient of variation. The approximation is local and is therefore best suited to moderate variability relative to the mean.

Consider now a change in the technology stock. An additional unit of $Tech_{k,it}$ shifts the conditional mean and the conditional variance at once, so the premium responds through both channels, and its total change follows from differentiating (8):

$$\frac{\partial RP_{it}}{\partial Tech_{k,it}} = \frac{\eta}{2}\left[\frac{1}{\mu_{1,it}} \cdot \frac{\partial \mu_{2,it}}{\partial Tech_{k,it}} - \frac{\mu_{2,it}}{\mu_{1,it}^2} \cdot \frac{\partial \mu_{1,it}}{\partial Tech_{k,it}}\right] \tag{9}$$

The mean path is the marginal benefit already defined in (2), since $\partial\mu_{1,it}/\partial Tech_{k,it} = -Benefit_{k,it}$. For the variance channel, write

$$g_{k,it} \equiv \frac{\partial \mu_{2,it}}{\partial Tech_{k,it}} \tag{10}$$

Here $g_{k,it}$, it is the variance analogue of $Benefit_{k,it}$, negative for a technology that compresses the spread of damages (Just and Pope, 1978). Substituting the two paths into (9) and reversing the sign, since the benefit is a reduction in the premium, gives the marginal risk premium benefit (MRPB):

$$MRPB_{k,it} \equiv -\frac{\partial RP_{it}}{\partial Tech_{k,it}} = -\frac{\eta}{2}\left[\frac{g_{k,it}}{\mu_{1,it}} + \frac{\mu_{2,it}}{\mu_{1,it}^2} Benefit_{k,it}\right] \tag{11}$$

The parameter η is imposed rather than estimated. It indexes the weight placed on the variability of damages: η = 0 corresponds to risk neutrality, and larger values evaluate uncertain damages more heavily (see Table 7). η is the damage-side counterpart of the coefficient of relative risk aversion—the same magnitude with mirrored curvature, since social cost is convex in damages where utility is concave in income—but it is measured against damages rather than income, so estimates from the income literature suggest a plausible range without providing a direct calibration. We therefore adopt the conventional interval η ∈ [1, 2] for sensitivity analysis and retain η = 1 as the baseline so as not to overstate the benefit. Since the marginal risk premium benefit is proportional to η, the baseline figures represent a lower bound, while the ordering of technologies does not depend on the value chosen.

Table 7. Interpretation of the coefficient of relative risk aversion

Relative risk aversion coefficients	Interpretations
$\eta = 0$	Risk neutrality
$\eta = 1$	Low degree of risk aversion
$\eta = 1.5$	Moderate degree of risk aversion
$\eta = 2$	High degree of risk aversion; uncertain damages weighted more heavily

Since η is imposed and $\mu_{1,it}$ and $Benefit_{k,it}$ are carried over from Section 3.1.1, what remains to be estimated in (11) is the second moment: the conditional variance $\mu_{2,it}$ and its response to each technology, $g_{k,it}$.

3.2. Econometric specifications

To empirically identify the key parameters defined in the conceptual framework in Section 3.1, this section specifies a set of estimation equations for the conditional mean and conditional variance of heatwave damage. Building on the resilience-based damage model of Choi et al. (2026), adaptation technologies are first linked to the physical dimension of HWRI, and the resulting index is then incorporated into the mean equation, while a separate variance equation is used to estimate technology-specific effects on damage uncertainty.

3.2.1. Step 1: Estimating the Effects of Adaptation Technologies on HWRI and its influence on Heatwave Damage

The first part of the empirical analysis examines how adaptation technologies affect the physical component of resilience and, through this channel, the expected level of heatwave damage. The physical dimension of HWRI is specified as a nonlinear function of the cumulative stock of four adaptation technologies: cooling fog system, cool roof, green roof & wall, shade canopy:

$$Phy_{it} = \delta_0 + \alpha_i + \sum_{k=1}^{4} \left(\delta_{1k} A_{k,it} + \delta_{2k} A_{k,it}^2\right) + \varepsilon_{it}\,, k = 1,2,3,4 \tag{12}$$

Here, $A_{k,it}$ denotes the cumulative stock of technology k in municipality i and year t, measured in units or areas depending on the technology type, δ_0 is a common intercept and α_i captures the municipality fixed effect. The error term ε_{it} represents unobserved factors affecting the damages not captured by the explanatory variables or fixed effects, and is assumed to satisfy $E(\varepsilon_{it} \mid Z_{it}) = 0$ and $Var(\varepsilon_{it} \mid Z_{it}) = \sigma_\varepsilon^2$, where Z_{it} denotes the set of explanatory variables in equation (12), consisting of the four technology stock variables and their squared terms. Including both linear and quadratic terms allow the marginal contribution of each technology to vary with its existing level of adoption. Accordingly,

$$\frac{\partial \widehat{PHY}_{it}}{\partial A_{k,it}} = \hat{\delta}_{1k} + 2\hat{\delta}_{2k} A_{k,it} \tag{13}$$

Since the economic, social, governance, and human components of HWRI are not directly determined by the adaptation technologies considered here, the predicted overall resilience index is constructed by combining these components with the predicted physical component: $\widehat{HWRI}_{it} = Econ_{it} + Gov_{it} + Human_{it} + Social_{it} + \widehat{Phy}_{it}$. Consequently, the marginal effect of technology k on the predicted HWRI is given by

$$\frac{\partial \widehat{HWRI}_{it}}{\partial A_{k,it}} = \hat{\delta}_{1k} + 2\hat{\delta}_{2k} A_{k,it} \tag{14}$$

To capture regional heterogeneity, the 17 South Korean provinces are split by a high-damage indicator D_i, corresponding to the top 25% of high-damage regions. Municipalities in the top quartile of the historical average damage distribution are assigned D_i=1, and the remaining municipalities are assigned D_i=0.

Using the predicted HWRI obtained above, the conditional mean equation relates log heatwave damage to predicted HWRI and the number of heatwave days, while allowing both effects to vary by a damage group. Heatwave damage is expressed in logarithmic form given its skewed distribution and to facilitate an elasticity-based interpretation with municipality (α_i) and year (λ_t) fixed effects, and HW_{it} the number of days with daily maximum temperature at or above 33°C.

$$\begin{aligned} \ln Y_{it} = \beta_0 + \beta_H ln\widehat{HWRI}_{it} + \theta_H\left(D_i \times \ln\widehat{HWRI}_{it}\right) + \beta_W HW_{it} \\ +\theta_W(D_i \times HW_{it}) + \alpha_i + \lambda_t + \varepsilon_{it} \end{aligned} \tag{15}$$

This specification corresponds to the mean equation implemented in the empirical model. Because the fitted values from the log-damage equation are expressed on the logarithmic scale, they are retransformed to obtain damage in monetary units. Let $\mu_{1,it} = E(Y_{it} \mid X_{it})$ denote the conditional mean. The marginal benefit (*MB*) of technology k is then obtained by linking the technology–resilience relationship to the conditional mean damage equation through the chain rule:

$$\frac{\partial \hat{\mu}_{1,it}}{\partial A_{k,it}} = \frac{\partial \hat{\mu}_{1,it}}{\partial \ln\hat{\mu}_{1,it}} \cdot \frac{\partial \ln\hat{\mu}_{1,it}}{\partial \ln\widehat{HWRI}_{it}} \cdot \frac{\partial \ln\widehat{HWRI}_{it}}{\partial \widehat{HWRI}_{it}} \cdot \frac{\partial \widehat{HWRI}_{it}}{\partial A_{k,it}} \tag{16}$$

which, after substitution, yields the marginal benefit of technology k as the implied reduction in expected damage as equation (16):

$$MB_{k,it} = -\frac{\partial \mu_{1,it}}{\partial A_{k,it}} = -\mu_{1,it}(\beta_H + \theta_H D_i)\frac{1}{H_{it}}\left(\delta_{1k} + 2\delta_{2k} A_{k,it}\right) \tag{17}$$

It shows that $MB_{k,it}$ is jointly determined by the expected damage level, the damage elasticity with respect to HWRI, and the technology's marginal contribution to resilience; a positive value represents the monetary value of avoided expected damage per unit of technology.

3.2.2. Step 2: Estimating the Effects of Adaptation Technologies on the Conditional

Variance of Heatwave Damage

While Step 1 characterizes how adaptation technologies affect the expected level of heatwave damage, technologies may also alter the uncertainty surrounding that damage — a dimension the mean equation alone cannot capture. Step 2 therefore estimates a separate variance equation for each technology, using the level-unit residual from the fitted mean equation as the outcome. The level-unit residual is constructed by taking the difference between observed damage and fitted damage $\hat{\mu}_{1,it}$ from the mean equation:

$$\hat{u}_{it} = Y_{it} - \hat{\mu}_{1,it}, \tag{18}$$

where Y_{it} is observed heatwave damage in KRW and $\hat{\mu}_{1,it}$ is the predicted damage in levels obtained from equation (19). Its square, $\hat{u}^2{}_{it}$, represents the square of the observation-specific deviation of realized damage from the estimated conditional mean and it can be interpreted as variance since the expected value of $\hat{u}^2{}_{it}$ is zero. Therefore, $\hat{u}^2{}_{it}$ can be used as the dependent variable in the variance equation:

$$\mu_{2,k,it} = E\left(\hat{u}^2{}_{it} \mid A_{k,it}, HW_{it}, i \right) \tag{19}$$

The conditional variance is estimated separately for each adaptation technology using an exponential specification, which ensures that the fitted variance remains positive:

$$\mu_{2,k,it} = \exp\left(\alpha_0 + \alpha_{ik} + \gamma_k A_{k,it} + \phi_k HW_{it}\right), k = 1,2,3,4, \tag{20}$$

where α_{ik} denotes municipality fixed effects, $A_{k,it}$ is the cumulative stock of technology k, and HW_{it} is the number of heatwave days. The marginal effect of technology k on the conditional variance of damage follows directly from the exponential link:

$$\frac{\partial \mu_{2,k,it}}{\partial A_{k,it}} = \gamma_k \mu_{2,k,it} \tag{21}$$

Here, the coefficient γ_k captures the effect of technology adoption on the conditional variance of heatwave damage. A negative value of γ_k indicates that greater adoption of technology k is associated with lower damage variability, whereas a positive value implies the opposite.

4. Results

4.1. Mean and variance equation results

Table 8 reports the estimation results for the conditional mean equation (equation 15). The coefficient on $\ln \widehat{HWRI}_{it}$ is negative and statistically significant ($\beta_H = -2.392,\ p < 0.001$), indicating that a 1% increase in predicted HWRI is associated with a 2.39% decrease in heatwave damage among municipalities in the lower-damage group. The coefficient on heatwave days ($\beta_W = 0.021,\ p < 0.001$) is statistically significant and positive, suggesting that the marginal effect of an additional heatwave day is larger in municipalities belonging to the top quartile of the historical damage distribution ($\theta_W =$

0.011, $p < 0.001$). Year fixed effects are included to account for common year-specific shocks over the 2016–2022 period, while municipality fixed effects control for time-invariant heterogeneity across municipalities.

Table 8. Mean Equation Regression Results

Variables	Parameters	Coeff. Estimates	Clustered Standard Errors
Intercept	β_0	18.36134***	0.289330
ln(HWRI)	β_H	-2.391582***	0.402384
ln(HWRI) × High-damage group	θ_H	0.819465	0.556371
Number of Annual heatwave days	β_W	0.021395***	0.001635
Annual heatwave days × High-damage group	θ_W	0.011453***	0.002386

Note: Municipality and year fixed effects are included. Standard errors are clustered at the municipality level. *, **, and *** indicate statistical significance at the 10%, 5%, and 1% levels, respectively.

Table 9 presents the results of the technology-specific conditional variance equations (equation 20). For all four technologies, the estimated coefficient on cumulative technology stock, γ_k, is negative and statistically significant, indicating that greater adoption is associated with a lower conditional variance of heatwave damage. Specifically, the effect is largest for cooling fog ($\gamma_1 = -0.027$), followed by green roofs/walls ($\gamma_3 = -0.020$), cool roofs ($\gamma_2 = -0.005$), and shade canopies ($\gamma_4 = -0.001$, all $p < 0.05$). The coefficient on heatwave days, ϕ_k, is consistently positive and statistically significant across all specifications, suggesting that greater heatwave exposure is associated with higher damage variability.

Taken together, the parameter estimates reported in Tables 8 and 9 supply the inputs for the risk-premium calculation that follows. The mean-equation coefficients characterize the expected-damage response, while the variance-equation coefficients capture technology-specific changes in conditional damage variance. These estimates are then combined to derive the risk premium and the risk-premium-adjusted benefit of each adaptation technology.

Table 9. Variance Equation Regression Results

Technologies	Parameters	Coefficients	Cluster SEs
Cooling Fog	γ_1	-0.027204***	0.008945
	ϕ_1	0.118651***	0.004101

Cool Roof	γ_2	-0.004841**	0.002238
	ϕ_2	0.121025***	0.003990
Green Roofs and Walls	γ_3	-0.019593***	0.007065
	ϕ_3	0.121128***	0.003979
Shade Canopy	γ_4	-0.001499***	0.000574
	ϕ_4	0.120010***	0.003995

Note: Municipality effects are included, and standard errors are clustered at the municipality level. *, **, and *** indicate statistical significance at the 10%, 5%, and 1% levels, respectively.

4.2. Marginal risk premium

Table 10 compares the conventional marginal benefit (MB) with the marginal risk-premium benefit (MRPB) for the four adaptation technologies. During the observed period, green roofs and walls generate the largest conventional MB, whereas cooling fog exhibits the largest MRPB and the largest risk-reduction benefit relative to its conventional MB (approximately 61.8%). This suggests that the technology providing the greatest reduction in expected damage is not necessarily the one providing the greatest value from reducing damage uncertainty. In particular, cooling fog can directly and rapidly reduce thermal stress through evaporative cooling, and previous studies have shown that its cooling effect remains substantial under extreme heat conditions (Desert et al., 2020). This characteristic is qualitatively consistent with the relatively large MRPB estimated for cooling fog, suggesting that its strong cooling effect under severe heat may contribute to limiting unusually large damage outcomes. A broadly similar pattern is observed in the SSP projections. While MRPB generally increases over time, cooling fog continues to show the largest MRPB, followed by green roofs and walls, cool roofs, and shade canopies. The increase is more pronounced in the later projection periods, particularly under the higher-forcing scenarios, indicating that the value of the risk-reduction component may become more important as future heatwave exposure intensifies. At $\eta = 1$, the implied risk premium amounts to 2.30 to 2.36 percent of expected damages across the four technologies.

Table 10. Marginal Benefit and Marginal Risk-Premium Benefit by Adaptation Technology

Period	Cooling Fog (per unit)		Cool Roof (per 100 m²)		Green Roofs And Walls (per 100 m²)		Shade Canopy (per unit)	
	MB	MRPB	MB	MRPB	MB	MRPB	MB	MRPB
2016 – 2022	1,088.46	672 (61.7%)	577.23	108 (18.7%)	1,459.57	456 (31.2%)	74.05	36 (48.6%)

Note 1: Unit = USD. MRRP is evaluated at $\eta = 1$.

Note 2: The 2016–2022 estimates are common to all scenarios because they are based on observed data.

Note 3: Figures in parentheses are MRPB as a percentage of MB.

Table 11. Marginal Risk-Premium Reduction Benefit by Technology and SSP Scenario

SSP scenario	Period	Cooling Fog (per unit)	Cool Roof (per 100 m²)	Green Roofs And Walls (per 100 m²)	Shade Canopy (per unit)
SSP1-2.6	2023–2030	1,306	240	948	73
	2031–2040	2,361	447	1,776	134
	2041–2050	3,741	705	2,778	212
SSP2-4.5	2023–2030	2,101	391	1,540	118
	2031–2040	2,678	499	1,959	150
	2041–2050	4,209	790	3,114	239
SSP3-7.0	2023–2030	1,613	297	1,160	90
	2031–2040	2,470	461	1,830	139
	2041–2050	7,858	1,539	6,073	453
SSP5-8.5	2023–2030	2,116	394	1,550	119
	2031–2040	2,422	455	1,794	136
	2041–2050	10,625	2,124	8,471	617

Note: Unit = USD MRRP is evaluated at $\eta = 1$.

4.3. BCR

4.3.1. Annual costs of resilience technologies

The annual cost parameters used in the benefit-cost analysis are summarized in Table 12. The costs are expressed in the same technology units used to calculate marginal benefits: per unit for cooling fog systems and shade canopies, and per 100 m² for cool roofs and green roofs and walls. Cooling fog systems have the highest annual cost, followed by green roofs and walls, cool roofs, and shade canopies. These annualized cost inputs are applied consistently when calculating both the BCR based only on expected-damage reductions and the risk-adjusted BCR that additionally incorporates the marginal risk-premium benefit. Unit costs are held constant in real terms throughout the projection horizon. Installation and maintenance costs may fall with technological progress and scale, or rise with input and labor costs, and we have no basis for projecting either. Holding them fixed isolates the effect of changing heat exposure on the benefit-cost ratio; the resulting ratios should be read as conditional on current cost conditions.

Table 12. Annual Cost Parameters Used in the Benefit-Cost Analysis

Technology	Unit	Annual cost (USD)
Cooling fog	per unit	7,910.16
Cool roof	per 100 m²	591.36
Green roofs and walls	per 100 m²	1,146.83

Shade canopy	per unit	145.21

Note: Annual cost corresponds to the marginal-cost input used in the BCR calculation. USD values are converted at KRW 1,415.90 per USD.

4.3.2 BCR with Risk-Premium

Accounting for the risk premium increases the benefit-cost ratio (BCR) of all adaptation technologies over the 2016–2022 period. However, the technology showing the largest relative increase in risk-adjusted benefits does not necessarily exhibit the highest cost-effectiveness, because the BCR reflects not only the magnitude of damage-reduction benefits but also the annual cost of each technology.

Green roofs and walls show the highest BCR both before and after accounting for the risk premium, increasing from 1.273 to 1.671 (+0.398). Cool roofs also show a notable improvement, with the BCR rising from 0.976 to 1.158. In particular, incorporating the risk premium moves the BCR for cool roofs from below to above the threshold of 1, indicating that risk adjustment can change the economic feasibility of a technology rather than simply increase the magnitude of its estimated benefits. In contrast, cooling fog systems show the largest relative increase in risk-adjusted benefits, approximately 61.8%, but their BCR increases only from 0.138 to 0.223 because of their relatively high unit cost and remains well below 1. Shade canopies similarly improve from 0.510 to 0.757 but do not exceed the benefit-cost threshold during the observed period. These differences indicate that the economic performance of adaptation technologies depends not only on the magnitude of their risk-reduction benefits but also on their underlying cost structures.

Across the future SSP scenarios, the relative ranking of technologies remains broadly similar. As heatwave exposure intensifies, however, MRPB contributes increasingly to total benefits, leading to a general increase in risk-adjusted BCRs over time.

Table 13. Benefit-Cost Ratios with and without Risk Adjustment by Adaptation Technology

Period	Cooling Fog (per unit)		Cool Roof (per 100 m²)		Green Roofs And Walls (per 100 m²)		Shade Canopy (per unit)	
	BCR without RP	BCR with RP	BCR without RP	BCR with RP	BCR without RP	BCR with RP	BCR without RP	BCR with RP
2016 – 2022	0.1376	0.223	0.9761	1.158	1.2727	1.671	0.5100	0.757

Table 14. Benefit Cost Ratios with Risk-Premium by Technology and SSP Scenario

SSP scenario	Period	Cooling Fog (per unit)	Cool Roof (per 100 m²)	Green Roofs And Walls (per 100 m²)	Shade Canopy (per unit)
SSP1-2.6	2023–2030	0.277	1.158	1.836	0.776
	2031–2040	0.427	1.624	2.703	1.232
	2041–2050	0.624	2.210	3.770	1.821
SSP2-4.5	2023–2030	0.394	1.526	2.486	1.126
	2031–2040	0.478	1.785	2.954	1.376
	2041–2050	0.690	2.392	4.120	2.030
SSP3-7.0	2023–2030	0.321	1.290	2.058	0.913
	2031–2040	0.443	1.660	2.774	1.283
	2041–2050	1.179	3.859	6.928	3.557
SSP5-8.5	2023–2030	0.394	1.520	2.488	1.126
	2031–2040	0.439	1.669	2.750	1.259
	2041–2050	1.553	5.027	9.237	4.722

Note: BCR = (MB + MRRP) / marginal cost, with MRRP evaluated at $\eta = 1$. A BCR greater than 1 indicates that the estimated marginal benefit exceeds the marginal cost..

5. Discussions

As shown above, accounting for the cost of risk raises the number of technologies that pass the benefit-cost test over the observation period (2016–2022) from one—green roofs and walls—to two, with cool roofs joining once the risk premium is counted (0.976 to 1.158); shade canopies follow later in the projection horizon, bringing the total to three under all four scenarios.

First, the level of the risk premium falls within the range reported in the existing literature. Expressed as a share of expected damages, it is 2.30 to 2.36 percent across the four technologies at $\eta = 1$, comfortably inside the 1 to 10 percent range that Markandya et al. (2019) report at the same degree of risk aversion. Although the conditional variance is estimated separately for each technology, the four estimates of the premium are nearly identical, because the technology term accounts for only a small part of the fitted variance: each equation is fitted to the same squared residuals and differs only in which technology stock enters as a regressor. The two magnitudes answer different questions. The first asks what fraction of expected damages the risk premium represents for a given damage distribution; the second asks how much a marginal unit of a technology reduces that premium, measured against the marginal benefit it delivers.

We are not aware of prior estimates of a marginal risk premium benefit of this kind. The fact that the risk-reducing effect of a technology can rival its effect on the mean, however, has been documented before. Traxler et al. (1995) find that in the post-green-revolution period, as breeding shifted toward pest and disease resistance, gains in mean yield slowed while yield risk fell—so that the technology worked more through the variance than through the mean. The same asymmetry drives our estimates: a marginal unit of technology lowers expected damages by 0.05 to 0.13 percent but lowers the conditional variance by 0.15 to 2.68 percent. Heat damages are heavily right-skewed, with a small number of extreme years accounting for much of the total variation, and if adaptation technologies operate most forcefully under extreme rather than ordinary conditions, their effect on the variance will exceed their effect on the mean. We do not test this mechanism directly, and how the effectiveness of each technology varies with the intensity of a heat wave remains an open question.

Second, accounting for the cost of risk does not change the economic ranking of technologies within a region. Nationally, the ranking—green roofs and walls, cool roofs, shade canopies, cooling fog—holds across all four scenarios and all periods, both before and after the risk premium is counted. At the provincial level, the ranking changes in only four or five provinces per scenario, and after the adjustment thirteen or fourteen provinces converge on the same ordering, so that the choice of technology becomes, if anything, more uniform across regions than it was before.

Every reordering takes the same form: cool roofs slip. They have the lowest ratio of marginal risk premium benefit to marginal benefit of the four technologies, so they gain least from the adjustment and lose their position wherever they had led narrowly. Cool roofs lower the thermal load on building surfaces continuously, delivering a steady benefit in ordinary conditions, whereas shade canopies and cooling fog are used intensively during heat waves and do more work at the extremes. The practical implication is that which technology to install can be decided much as before, but how much to allocate across regions may depend on whether the cost of risk is counted.

Third, accounting for the cost of risk widens the gap between scenarios considerably. Counting only the reduction in expected damages, the benefit-cost ratio under SSP5 is 1.3 to 1.4 times that under SSP1; once the risk premium is included, it rises to between 2.3 and 2.6. More heat wave days raise both expected damages and the conditional variance, and our estimates put the variance response the larger of the two. The choice of emissions pathway can therefore decide the verdict. A technology whose benefit-cost ratio falls below one under a low-emissions pathway may rise above it under a high-emissions pathway, and the gap between the two widens once the cost of risk is counted. An appraisal built on a single scenario that presumes mitigation targets are met will not capture what adaptation is worth if mitigation is delayed; adaptation projects are better evaluated against several emissions pathways.

Table 15. Benefit–cost ratios under SSP1 and SSP5 with and without the risk premium, 2041–2050

Scenarios	Cooling Fog (per unit)	Cool Roof (per 100 m²)	Green Roofs And Walls (per 100 m²)	Shade Canopy (per unit)
BCR without RP				
SSP1	0.15	1.02	1.35	0.36
SSP5	0.21	1.44	1.85	0.47

Scenarios	Cooling Fog (per unit)	Cool Roof (per 100 m²)	Green Roofs And Walls (per 100 m²)	Shade Canopy (per unit)
SSP5/SSP1	1.39	1.41	1.37	1.29
BCR with RP				
SSP1	0.62	2.21	3.77	1.82
SSP5	1.55	5.03	9.24	4.72
SSP5/SSP1	2.49	2.27	2.45	2.59

Judged on expected benefits alone, the relative value of adaptation looks much the same whatever emissions pathway one assumes. Once the cost of risk enters, the benefit under a high-emissions pathway is more than double than under a low-emissions one. An adaptation plan built on a single scenario therefore risks overlooking a substantial part of what these technologies are worth in a world where mitigation is delayed.

6. Conclusions

This study extends the benefit–cost appraisal of urban heatwave adaptation to include the value of reduced uncertainty. Using a panel of all 229 Korean municipalities for 2016–2022, we estimate conditional mean and variance equations for heat damages and convert the technology-induced reduction in damage variability into a marginal risk premium benefit. Counting this benefit raises the number of technologies that pass the benefit–cost test from one to two over the observation period, and to three in the projection horizon. Green roofs and walls remain the strongest performer throughout; cool roofs move from 0.976 to 1.158, crossing the threshold only once risk is priced.

Two implications follow for practice. First, appraisal guidelines that presume risk neutrality can understate the case for adaptation, and the understatement is largest precisely where it matters most—for technologies whose benefit–cost ratios sit near unity, where counting the cost of risk decides the verdict. Second, because the value of adaptation depends heavily on the emissions pathway assumed, an appraisal built on a single scenario will misstate what these technologies are worth; several pathways should be carried through the calculation. More generally, local governments comparing adaptation options have reason to weigh not only how much a technology lowers damages on average, but how much it stabilizes them.

Two qualifications bear on these results. In this paper, the risk aversion parameter is imposed rather than estimated: it governs the curvature of utility over damages, so estimates obtained from income or consumption do not carry over, and no method is currently available for recovering the risk preferences of a local government from observed behavior. We report a sensitivity range together with the minimum degree of risk aversion at which each verdict changes, but the magnitude of the risk premium benefit remains proportional to a parameter we have assumed. The identification of the conditional variance is also thin. Heat damages have a pronounced right tail and 2018 alone accounts for roughly two-thirds of the total squared residual variation—the feature that makes the risk premium worth pricing is the same one that leaves the variance equation sensitive to a handful of events. For some technologies the resulting estimate falls short of conventional significance. A related concern applies to the projections: the heat-day coefficient is identified over the range observed between 2016 and 2022, while a substantial fraction of the values projected for the 2040s lies outside it. The projected benefits are best read as an upper bound, with policy judgments resting on the observed period and the near term.

Each of these points to work worth doing. Most pressing is to recover the risk preference parameter from data. The fiscal choices local governments make—the size of disaster reserve funds, whether to purchase disaster insurance, how contingency budgets are used—reveal how they trade expected cost against risk, and could support estimation rather than assumption. Sharpening the variance estimates calls for finer temporal resolution: daily observations, or data organized around individual heat events, would capture considerably more variation than an annual panel, and estimating directly how technologies shift the upper quantiles of the damage distribution would provide evidence independent of the moment-based framework. Finally, the scope could usefully be widened. Local governments face correlated risks across several hazards, and a risk premium computed jointly would be more accurate than the sum of hazard-by-hazard calculations. Physical adaptation is also not the only way to reduce the cost of bearing risk; placing disaster insurance and reserve accumulation alongside adaptation investment in a common framework would speak more directly to how municipalities actually manage risk.

What the paper contributes, then, is a way of carrying the second moment of the damage distribution into project appraisal. Work on risk aversion in benefit-cost analysis has generally taken the damage distribution as given, while the moment-based literature on how inputs affect output variance has developed around agricultural production decisions. Joining the two yields a measure of how much a marginal unit of an adaptation technology reduces the risk premium—and, with it, evidence that counting only the reduction in expected damages understates what these technologies are worth, unevenly across regions.

This work was supported by Korea Environment Industry &Technology Institute (KEITI) through "Climate Change R&D Project for New Climate Regime.", funded by Korea Ministry of Climate, Energy and Environment. (MCEE) (RS-2022-KE002102)

References

Antle, J. M. (1983). Testing the stochastic structure of production: A flexible moment-based approach. *Journal of Business & Economic Statistics*, 1(3), 192–201.

Arrow, K. J., & Lind, R. C. (1970). Uncertainty and the evaluation of public investment decisions. *American Economic Review*, 60(3), 364–378.

Barreca, A., Clay, K., Deschênes, O., Greenstone, M., & Shapiro, J. S. (2016). Adapting to climate change: The remarkable decline in the US temperature-mortality relationship over the twentieth century. *Journal of Political Economy*, 124(1), 105–159.

Choi, Y., Lee, S., Choi, W., Kim, D., Kim, K., & An, D. (2026). Evaluating heatwave adaptation technologies through municipal climate resilience pathways: Evidence from South Korea. *Mitigation and Adaptation Strategies for Global Change* (currently under review).

Coronese, M., Lamperti, F., Keller, K., Chiaromonte, F., & Roventini, A. (2019). Evidence for sharp increase in the economic damages of extreme natural disasters. *Proceedings of the National Academy of Sciences*, 116(43), 21450–21455. https://doi.org/10.1073/pnas.1907826116

Desert, A., Naboni, E., & Garcia, D. (2020). The spatial comfort and thermal delight of outdoor misting installations in hot and humid extreme environments. *Energy and Buildings, 224*, 110202. https://doi.org/10.1016/j.enbuild.2020.110202

Di Falco, S., & Chavas, J.-P. (2009). On crop biodiversity, risk exposure, and food security in the highlands of Ethiopia. *American Journal of Agricultural Economics*, 91(3), 599–611. https://doi.org/10.1111/j.1467-8276.2009.01265.x

HM Treasury. (2026). *The Green Book: Central government guidance on appraisal and evaluation*. London: HM Treasury.

Hochrainer-Stigler, S., Keating, A., Handmer, J., & Ladds, M. (2018). Government liabilities for disaster risk in industrialized countries: A case study of Australia. *Environmental Hazards*, 17(5), 418–435. https://doi.org/10.1080/17477891.2018.1426554

Just, R. E., & Pope, R. D. (1978). Stochastic specification of production functions and economic implications. *Journal of Econometrics*, 7(1), 67–86.

Kim, K., & Chavas, J.-P. (2003). Technological change and risk management: An application to the economics of corn production. *Agricultural Economics*, 29(2), 125–142. https://doi.org/10.1016/S0169-5150(03)00081-1

Kind, J., Botzen, W. J. W., & Aerts, J. C. J. H. (2017). Accounting for risk aversion, income distribution and social welfare in cost-benefit analysis for flood risk management. *WIREs Climate Change*, 8(2), e446.

Lee, G. E., & Cho, H. N. (2024). Analysis and improvement of regional heatwave policy through in-depth interviews with public officials (in Korean with English abstract). *Journal of Climate Change Research*, 15(6), 1051–1062. https://doi.org/10.15531/KSCCR.2024.15.6.1051

Markandya, A., De Cian, E., Drouet, L., Polanco-Martínez, J. M., & Bosello, F. (2019). Building risk into the mitigation/adaptation decisions simulated by integrated assessment models. *Environmental and Resource Economics*, 74(4), 1687–1721.

Newbold, S. C., Griffiths, C., Moore, C., Wolverton, A., & Kopits, E. (2013). A rapid assessment model for understanding the social cost of carbon. *Climate Change Economics*, 4(1), 1350001. https://doi.org/10.1142/S2010007813500012

Office of Management and Budget. (2023). *Circular A-4: Regulatory analysis*. Washington, DC: Executive Office of the President.

Pyon, H. S. (2022). *Policy proposal for the effectiveness and promotion of rooftop greening* (Chungbuk Focus No. 207). Cheongju: Chungbuk Research Institute.

Traxler, G. J., Falck-Zepeda, J. I., Ortiz-Monasterio, R. J. I., & Sayre, K. (1995). Production risk and the evolution of varietal technology. *American Journal of Agricultural Economics*, 77(1), 1–7.

Weitzman, M. L. (2009). On modeling and interpreting the economics of catastrophic climate change. *Review of Economics and Statistics*, 91(1), 1–19.

Wiyanti, A., & Halimatussadiah, A. (2021). Are disasters a risk to regional fiscal balance? Evidence from Indonesia. *International Journal of Disaster Risk Science*, 12(6), 839–853.

Appendix A.1. Marginal Benefits and Benefit-Cost Ratios with and without Risk Premium across SSP Scenarios

SSP scenario	Technology	Period	MB (USD)	BCR without RP	MRPB (USD)	BCR with RP
SSP1-2.6	Cooling fog	2016–2022	1,088.46	0.1376	672.35	0.2226
		2023–2030	881.68	0.1115	1,306.19	0.2766
		2031–2040	1,014.59	0.1283	2,361.17	0.4268
		2041–2050	1,195.54	0.1511	3,741.25	0.6241
	Cool roof	2016–2022	577.23	0.9761	107.75	1.1583
		2023–2030	445.19	0.7528	239.55	1.1579
		2031–2040	512.75	0.8671	447.36	1.6236
		2041–2050	601.75	1.0176	705.25	2.2102
	Green roof/wall	2016–2022	1,459.57	1.2727	456.41	1.6707
		2023–2030	1,157.88	1.0096	947.92	1.8362
		2031–2040	1,323.42	1.1540	1,776.30	2.7029
		2041–2050	1,545.08	1.3473	2,778.12	3.7697
	Shade canopy	2016–2022	74.05	0.5100	35.91	0.7573
		2023–2030	40.18	0.2767	72.51	0.7761
		2031–2040	45.27	0.3117	133.69	1.2324
		2041–2050	52.84	0.3639	211.62	1.8212
SSP2-4.5	Cooling fog	2016–2022	1,088.46	0.1376	672.35	0.2226
		2023–2030	1,012.09	0.1279	2,101.36	0.3936
		2031–2040	1,104.12	0.1396	2,677.66	0.4781
		2041–2050	1,250.07	0.1580	4,209.07	0.6901
	Cool roof	2016–2022	577.23	0.9761	107.75	1.1583
		2023–2030	510.94	0.8640	391.48	1.5260
		2031–2040	555.95	0.9401	499.39	1.7846
		2041–2050	624.20	1.0555	790.26	2.3919
	Green roof/wall	2016–2022	1,459.57	1.2727	456.41	1.6707
		2023–2030	1,310.12	1.1424	1,540.33	2.4855
		2031–2040	1,428.17	1.2453	1,959.46	2.9539
		2041–2050	1,611.17	1.4049	3,114.03	4.1202
	Shade canopy	2016–2022	74.05	0.5100	35.91	0.7573
		2023–2030	45.52	0.3135	117.95	1.1258
		2031–2040	49.29	0.3394	150.48	1.3757
		2041–2050	55.95	0.3853	238.76	2.0296

Appendix A.2. Marginal Benefits and Benefit-Cost Ratios with and without Risk Premium across SSP Scenarios (continued)

SSP scenario	Technology	Period	MB (USD)	BCR without RP	MRPB (USD)	BCR with RP
SSP3-7.0	Cooling fog	2016–2022	1,088.46	0.1376	672.35	0.2226
		2023–2030	924.40	0.1169	1,612.81	0.3208
		2031–2040	1,037.04	0.1311	2,470.02	0.4434
		2041–2050	1,471.03	0.1860	7,857.96	1.1794
	Cool roof	2016–2022	577.23	0.9761	107.75	1.1583
		2023–2030	465.25	0.7868	297.30	1.2895
		2031–2040	520.81	0.8807	460.92	1.6601
		2041–2050	743.10	1.2566	1,538.86	3.8589
	Green roof/wall	2016–2022	1,459.57	1.2727	456.41	1.6707
		2023–2030	1,200.19	1.0465	1,159.52	2.0576
		2031–2040	1,351.04	1.1781	1,829.99	2.7738
		2041–2050	1,871.86	1.6322	6,073.13	6.9278
	Shade canopy	2016–2022	74.05	0.5100	35.91	0.7573
		2023–2030	42.37	0.2918	90.15	0.9126
		2031–2040	46.97	0.3235	139.36	1.2832
		2041–2050	63.17	0.4351	453.30	3.5568
SSP5-8.5	Cooling fog	2016–2022	1,088.46	0.1376	672.35	0.2226
		2023–2030	1,000.79	0.1265	2,115.62	0.3940
		2031–2040	1,049.75	0.1327	2,421.61	0.4388
		2041–2050	1,662.99	0.2102	10,624.93	1.5534
	Cool roof	2016–2022	577.23	0.9761	107.75	1.1583
		2023–2030	505.22	0.8543	393.89	1.5204
		2031–2040	531.58	0.8989	455.10	1.6685
		2041–2050	849.11	1.4359	2,123.82	5.0273
	Green roof/wall	2016–2022	1,459.57	1.2727	456.41	1.6707
		2023–2030	1,303.48	1.1366	1,550.04	2.4882
		2031–2040	1,359.40	1.1854	1,794.23	2.7499
		2041–2050	2,122.65	1.8509	8,470.95	9.2373
	Shade canopy	2016–2022	74.05	0.5100	35.91	0.7573
		2023–2030	44.84	0.3088	118.60	1.1256
		2031–2040	46.51	0.3203	136.30	1.2590
		2041–2050	68.28	0.4702	617.37	4.7219

Note: MB denotes the marginal expected-damage reduction benefit, and MRPB denotes the marginal risk-premium reduction benefit. BCR without RP = MB / marginal cost; BCR with RP = (MB + MRPB) / marginal cost. MRPB is evaluated at $\eta = 1$ for all SSP scenarios. The 2016–2022 values are common across